

Semiflexible polymer chains on the square lattice: Numerical study of critical exponents

Ivan Živić*

University of Kragujevac, Faculty of Science, R. Domanovića 12, 34000 Kragujevac, Serbia

Sunčica Elezović-Hadžić† and Sava Milošević‡

University of Belgrade, Faculty of Physics, P.O. Box 44, 11001 Belgrade, Serbia

(Received 10 June 2018; revised manuscript received 14 August 2018; published 21 December 2018)

We have studied the statistics of semiflexible linear polymer chains modeled by self-avoiding random walk (SAW) on the square lattice. We applied the PERM Monte Carlo simulation method to sample the polymer chain configurations for SAWs up to 2000 steps. Varying the stiffness parameter s of the chain we have calculated numerically the critical exponents ν (associated with the mean squared end-to-end distance of polymer chain) and γ (associated with the partition function of polymer chain system), as well as the growth constant μ . We find a clear numerical evidence that, in the studied region of s , both critical exponents (ν and γ) do not depend on polymer flexibility. Besides, for moderately flexible chains, we show that the growth constant μ displays a linear dependence on the stiffness parameter s . We discuss and relate our findings to those obtained previously for Euclidean and fractal polymer containers.

DOI: [10.1103/PhysRevE.98.062133](https://doi.org/10.1103/PhysRevE.98.062133)**I. INTRODUCTION**

The self-avoiding walk (SAW) is a random walk that must not contain self-intersections, and it has been accepted as canonical model of linear polymer chains [1]. The pure SAW is a good model for perfectly flexible polymer, where one ignores the apparent rigidity of real polymer, and consequently, associates the same weight factor (fugacity) to each step of SAW. Statistics of flexible SAW chains has been widely studied for continuous and discrete containers of polymers [2]. However, in most real cases the polymers are semiflexible (with various degree of stiffness), such as DNA biopolymers [3] as well as a wide class of synthetic polymers [4]. Recently, the significant attention has been devoted to theoretical and experimental research [5–7] of stiffness properties of isolated semiflexible polymers with the so-called bottle-brush architecture. The latter can be envisaged as macromolecules that consist of a long backbone chain along which smaller side-chains are attached [8,9], with an important feature that changing the length and grafting density of attached chains the stiffness of bottle-brush polymers may be varied over a wide range. The measure of polymer stiffness is the persistence length ℓ_p (average length of straight parts of a chain), and hence various types of semiflexible SAW models have been invented, with a focus on the persistence length behavior. The stiffness property enlarges the persistence length, so that for stiff enough chains ℓ_p becomes comparable with the polymer length L . In the limit of very stiff chains $\ell_p \gg L$ holds, and the polymer takes the rigid-rod-like form. In the continuous space models the polymer stiffness is modeled by constraining

the angle between consecutive bonds of polymer or assigning an extra energy to each bend of the chain, while in the lattice models an additional statistical weight is introduced for each turn in the walk.

Theoretical investigation of semiflexible chain molecules was initiated by Flory [10] in a study of polymer crystallization, where an energy penalty was added to each bend of the polymer chain to model the polymer inflexibility (see also the pioneering study of chain molecules [11]). The real polymer system is almost always consisting of collection of polymer chains, but because of complexity of such a system the study of single-chain statistics has been frequently applied, as a requisite step towards understanding the statistics of many-chain systems. The first model of single semiflexible polymer (that includes the excluded volume effect) has been the biased (or persistent) SAW model, where the probability to make the next step is different for straight steps (which do not change the SAW direction) and bending steps (those that change the SAW direction). For this SAW model scaling properties of semiflexible polymers in the so-called rod-to-coil crossover region have been studied on two- and three-dimensional Euclidean lattices [12–15]. The same problem of conformational rod-to-coil transition of stiff polymer chain has also been studied for directed SAW model, which has been solved exactly [16–18] on hypercubic lattices in arbitrary dimension $d \geq 2$. The persistent SAW model has been enhanced by introducing an energy penalty ϵ for each turn of the walk [19,20]. Accordingly, for $\epsilon < 0$ the probability for SAW bends is enlarged favoring more flexible SAW states (with more bends), for $\epsilon \ll 0$ the super-flexible polymer chain emerges [21], while the case $\epsilon > 0$ favors the stiffer chain states (with less bends).

Investigation of asymptotic properties (for large number of steps) of various types of self-avoiding walk models, appears to belong to category of demanding problems in the critical

*ivanz@kg.ac.rs

†suki@ff.bg.ac.rs

‡savam@ff.bg.ac.rs

phenomena studies. To comprehend various features of semiflexible polymers within the SAW model numerous studies have been performed. One of the main issues in semiflexible polymer model studies has been to answer the question if the critical exponents depend on polymer stiffness and whether different self-avoiding-type models have the same values for critical exponents (belong to the same universality class) for the same polymer flexibility. In corresponding studies universality arguments, as well as results of approximate and extrapolation methods for similar models, suggest that critical exponents on regular (Euclidean) lattices should not be affected by the value of polymer stiffness. Besides, in the recent Monte Carlo studies of SAWs on the simple cubic and square lattice [20,22] the rescaled mean square end-to-end distance was analysed for a wide range of polymer stiffness. The obtained results, in the limit of very long chains, support the prediction that end-to-end distance critical exponent ν on regular lattices remains unaltered upon the changes of polymer stiffness. However, research on fractal structures [19,23–25] revealed that geometrical critical exponents are stiffness dependent, for a wide range of flexibility. Since, to the best of our knowledge, there have been no detailed and precise numerical studies of semiflexible SAW model on Euclidean lattices to confirm the expected behavior of critical exponents, we have been motivated to perform such a study on the square lattice. Thus, in this paper we report on results obtained by performing numerical study of geometrical critical exponents by applying the pruned-enriched Rosenbluth method (PERM) to simulate semiflexible SAWs on the square lattice. We have calculated the end-to-end distance critical exponents ν (associated with the mean squared end-to-end distance of polymer chain) and the entropic critical exponents γ (associated with the total number of different polymer configurations), as well as the growth constant μ , for semiflexible SAWs. Besides, we have performed our calculations for various degrees of polymer stiffness s , to study stiffness dependence of the geometrical critical exponents. Furthermore, we have explored the impact of polymer stiffness on statistics of SAW in various types of polymer containers.

This paper is organized as follows. We define the semiflexible SAW model on the square lattice in Sec. II, where we also present the framework of the PERM Monte Carlo approach for sampling linear polymer chains with relevant flexibility. In Sec. III we describe the way of numerical evaluation of geometrical critical exponents (ν and γ) and the growth constant μ for stiff polymers. In the same section we expose and discuss the obtained specific results. Finally, in Sec. IV we give a short summary of our work and pertinent conclusions.

II. MODEL AND METHOD

To describe stiffness of a polymer chain, we introduce the Boltzmann factor $s = e^{-\epsilon/k_B T}$, where ϵ is an energy barrier associated with each bend of the SAW path, and k_B is the Boltzmann constant. The case $s < 1$ ($\epsilon > 0$) corresponds to stiffer polymer chains, while the case $s > 1$ ($\epsilon < 0$) brings out chains with enhanced flexibility. The two limiting cases $s \rightarrow 0$ and $s \rightarrow \infty$ correspond to the so-called rigid-rod-like and super-flexible chain, respectively, whereas completely flexible chain coincides with the case $s = 1$ ($\epsilon = 0$). Within the model

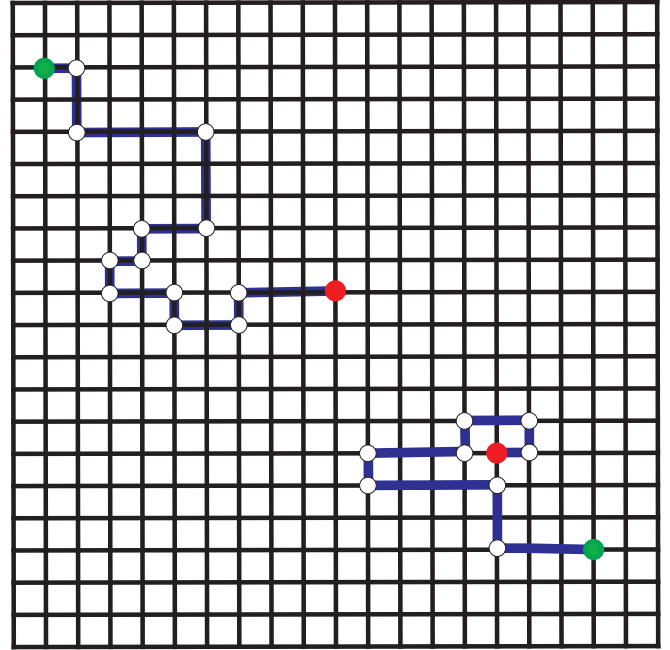


FIG. 1. Two examples of SAW path (blue line) on the square lattice. Full green circles are starting and red ones are ending points of the SAW. Empty circles denote turn points of the walker (that is, bends of the SAW path), to which we associate the Boltzmann factor $s = e^{-\epsilon/k_B T}$, where ϵ is the energy related to polymer bends. Thus, for example, the left SAW configuration has length $N = 24$ with $N_b = 12$ bends. Its RR weight is $W_{24} = (4 \times 3^{15} \times 2 \times 3^7) s^{12} = 251048476872 s^{12}$, in accord with Eq. (7). The right SAW configuration is an example of trapped walker (the polymer growth, with $N_b = 8$ bends, is stopped after $N = 18$ steps).

described the persistence length is a function of s . For $s \geq 1$ (when bends are favorable) it is equal to the lattice constant $\ell_p(s) \sim 1$, while for $s < 1$ it behaves as $\ell_p(s) \sim s^{-1}$.

If we assign the weight x to each step of the SAW, then the weight of a walk having N steps, with N_b bends, is $x^N s^{N_b}$ (see Fig. 1), and, consequently, the generating function for SAWs of all possible length has the form

$$G(x, s) = \sum_{N=1}^{\infty} Z_N(s) x^N. \quad (1)$$

Here

$$Z_N(s) = \sum_{N_b=0}^{N-1} C(N, N_b) s^{N_b} \quad (2)$$

is the partition function for an N -step SAW system, while $C(N, N_b)$ is the number of N -step SAWs having N_b bends. For large N it is expected that the above sum displays the following power-law behavior:

$$Z_N \sim \mu^N N^{\gamma-1}, \quad (3)$$

where γ and μ are the entropic critical exponent and the growth constant, respectively, and may depend on polymer flexibility s . For fully flexible polymers ($s = 1$) the critical exponent γ is universal on the Euclidean lattices, with the

exact value $\gamma = 43/32$ [26,27] for dimension $d = 2$, while μ is a lattice dependent quantity.

To describe metric properties of SAWs we define the mean squared end-to-end distance for an N -step semiflexible SAW system

$$\langle R_N^2(s) \rangle = \frac{1}{Z_N(s)} \sum_{N_b=0}^{N-1} \rho(N, N_b) s^{N_b}, \quad (4)$$

where

$$\rho(N, N_b) = \sum_{i=1}^{C(N, N_b)} r_i^2 = \sum_{i=1}^{C(N, N_b)} (x_i^2 + y_i^2 + z_i^2), \quad (5)$$

and r_i is the Euclidean distance between end points of an N -step SAW having N_b bends. For large N , we expect the following scaling behavior:

$$\langle R_N^2 \rangle \sim N^{2\nu}, \quad (6)$$

where ν is the end-to-end distance critical exponent, that in general might depend on stiffness parameter s . For fully flexible ($s = 1$) two-dimensional SAWs the critical exponent ν is universal and equal to $3/4$. In addition, in this model the persistence length is defined as an average number of steps between two consecutive bends $\ell_p = \lim_{N \rightarrow \infty} \frac{N}{\langle N_b \rangle}$, where $\langle N_b \rangle = \frac{1}{Z_N} \sum_{N_b=0}^{N-1} N_b C(N, N_b) s^{N_b}$ is the mean number of bends in an ensemble of SAW chains of length N , which have been numerically studied on Euclidean lattices [21], as a function of bending energy.

Our goal is to calculate numerically ν , γ , and μ , for $s \neq 1$, on the square lattice to establish whether they depend on s . To this end we generate sets of SAW samples with various polymer flexibility s . To create SAWs of different lengths we apply the pruned-enriched Rosenbluth-Rosenbluth method (PERM) [28], which is an upgraded version of the Rosenbluth-Rosenbluth (RR) method [29] for growing chains of different lengths, and here we present a brief review of both approaches, that is, of the original and upgraded.

We start with the basic ideas of the RR method, which is a biased kinetic growing walks algorithm on a lattice. In this method the SAW chain grows step by step, starting from an arbitrary lattice site (this growth process, from a start, we call the tour). The new step is appended to an existing chain, so that it is chosen randomly from the set of all possible steps toward previously unvisited neighboring sites. We let the walker repeat the step adding procedure up to predetermined maximal chain length N_{\max} . In the case when, after some number of steps N (smaller than N_{\max}), all neighboring sites are occupied (the walker is trapped) the chain growth is stopped and we start a new tour from the origin, with $N = 0$. When the walk attains the maximal length N_{\max} we finish the SAW simulation, and in that case we say that this tour is successful. In practice we generate n_T successful tours, creating the same number of SAWs of the length N_{\max} . We note that consecutive SAW parts, created during the growth process within one tour, may be used as samples for shorter SAWs (of lengths less than the maximal one achieved in this tour). Clearly, the number of N -step SAW chains with $N < N_{\max}$ is larger or equal to n_T since some walks have been trapped before reaching the full

length N_{\max} (i.e., the number of total tours is greater or equal to the number of successful ones).

Random walks created in RR method are biased, since previously visited neighboring sites are excluded from the next step random choice. To take the bias into account we assign different statistical weights to sampled N -step walks. For an N -step semiflexible SAW the RR weight is

$$W_N = \prod_{i=0}^{N-1} n_f(i) s^{(1-\cos\theta_{i,i+1})} \\ = W_{N-1} n_f(N-1) s^{(1-\cos\theta_{N-1,N})}, \quad (7)$$

where $n_f(i)$ is the number of free (previously non-occupied by the walk) neighboring sites after i steps in the growing SAW process (also called the atmosphere of the walk [30]), and $\theta_{i,i+1}$ is the angle between the two consecutive steps. The starting values for these quantities are $n_f(0) = 4$ and $\theta_{0,1} = 0$.

The partition function for an N -step SAW system is calculated as an average of the weights given by Eq. (7), that is

$$Z_N = \langle W_N \rangle = \frac{1}{s_0} \sum_{i=1}^{s_N} [W_N]_i. \quad (8)$$

In the above sum, the number of terms is equal to the number of N -step SAW samples s_N . It should be emphasized that, to obtain the correct result for Z_N , this sum should be averaged over the number of starting SAWs s_0 , not over the number of N -step SAW samples s_N [31,32]. Since the number s_0 includes SAWs that might be trapped before attaining the length N (their weight is zero), the relation $s_0 \geq s_N$ holds in the RR method. In the high temperature region (i.e., for an athermal system) Z_N coincides with the total number C_N of distinct N -step SAWs, so that the RR algorithm might be conceived as an approximate method for C_N calculation. Apart from Z_N (which provides information about the entropic critical exponent γ) in our focus of interest is the mean squared end-to-end distance $\langle R_N^2 \rangle$, determined by the metric critical exponent ν . Within the RR method the latter can be evaluated as

$$\langle R_N^2 \rangle = \frac{\sum_{i=1}^{s_N} [W_N]_i [R_N^2]_i}{\sum_{i=1}^{s_N} [W_N]_i}, \quad (9)$$

where $[R_N^2]_i$ is the squared end-to-end distance of i -th sample of SAW containing N -step, with the weight $[W_N]_i$ calculated in accord with Eq. (7).

In the implementation of RR method two problems emerge when we try to generate polymers consisting of large number of monomers N . The first one emerges when longer chains are simulated and an immense number of starting walks become trapped before attaining the desired length (i.e., the rate of successful tours decreases with N). In this situation sampling of longer SAWs appears to be inefficient, and an exponential attrition of SAW samples occurs. The second problem, in addition to the large number of low weight SAW samples, is that a few samples with a very large weight are generated. These rare configurations predominantly determine the mean value of the weights [given by Eq. (8)], and distort ensemble statistics producing a decidedly high dispersion in the weights. These two side effects of RR method make it inefficient for longer SAWs simulation.

To eliminate above problems two improvements of RR algorithm have been introduced: enriching the walks with high weight, and pruning the low weight walks in a systematic way [28]. The new algorithm has been called the PERM (pruned and enriched Rosenbluth method). Accordingly, one defines the two thresholds W_N^- and W_N^+ , for an N -step SAW weight W_N , which are incessantly updated during the chain growth. If $W_N > W_N^+$ one replaces the current configuration with two identical copies (clones), each having the half of the original weight $W_N \rightarrow W_N/2$. This transformation is called enrichment. Now, one of two clones continues to grow, while the second one waits in a stack until the first clone finishes its growth. However, the low weight configurations $W_N < W_N^-$, are eliminated with the probability 1/2, and if the SAW survives one doubles its weight $W_N \rightarrow 2W_N$. This process is called the pruning. In this way one keeps the weights W_N close to the window $[W_N^-, W_N^+]$, eliminating configurations with low and high weights. It is important to perceive that both enrichment and pruning do not change the values of averages defined by Eqs. (8) and (9). Only the number of terms s_N in the sums may be changed, but the sums are not disturbed. The choice of W_N^- and W_N^+ is fairly arbitrary, but the efficiency of the method depends on its choice. It is plausible to choose the values for W_N^- and W_N^+ to be comparable with the mean $\langle W_N \rangle$. Various choices may be done, and here we go for

$$W_N^- = c_- \langle W_N \rangle \left(\frac{s_N}{s_0} \right)^2, \quad W_N^+ = c_+ \langle W_N \rangle \left(\frac{s_N}{s_0} \right)^2, \quad (10)$$

where coefficients c_- and c_+ are constant [33]. In particular, it has been set out $c_- = 1/5$ and $c_+ = 1$, since this choice provides that the number of samples s_N is approximately the same for polymers of different length N .

III. SIMULATION RESULTS AND DISCUSSION

We have simulated semiflexible polymer chains on the square lattice for various values of polymer flexibility. The set of values for stiffness parameter ($s = 0.2, 0.3, 0.4, 0.6, 0.8, 1, 1.5, 2, 3, 4$ and 5) have been chosen in such a way that the $\log(s)$ scale is almost linear. Using the method described in the previous section, for each specific s we performed a large number of Monte Carlo simulations, for polymers of the maximal length $N_{\max} = 2000$. The simulation process begins with the SAW that starts its growth from an arbitrary site of the lattice, in accordance with the PERM algorithm. Within each simulation tour polymer chains of different lengths N are created. All SAWs generated within one tour are correlated (because of the enrichment), while those belonging to different tours are independent [28]. Some tours are terminated before the SAWs (generated within the tour) reach the maximal length N_{\max} . The tour is successful when length of simulated SAW chain attains the given maximal value N_{\max} . At that milestone we stop the possible further simulation of chains (with lengths $N > N_{\max}$), finishing the tour simulating only SAWs with $N \leq N_{\max}$. We repeat the simulating process (from starting point) until the preset number of successful tours is carried out. Within a generated SAW of length N , successive parts (of the lengths less than N) are also used as members of shorter SAWs ensembles. During the simulations, for each SAW configuration of length N , generated by the PERM,

we record the weight $[W_N]_i$ and the corresponding squared end-to-end distance $[R_N^2]_i$ ($i = 1, 2, \dots, s_N$). Then, for n_T successful simulation tours, the number of ensemble members of length N ($N \leq N_{\max}$) is $s_N = k_N n_T$, where $k_N > 1$ in practice. For one simulation session, consisting of n_T successful tours, the choice of W_N^- and W_N^+ , given by Eq. (10), ensures that the number of samples s_N of different length N is almost the same. That is, the coefficient k_N does not depend on N , but it is a function of the maximal length N_{\max} and the stiffness parameter s : $k_N = k_N(N_{\max}, s)$. For fixed s , $k_N(N_{\max}, s)$ increases with N_{\max} almost linearly (for instance, $k_N(1000, 1) \simeq 69$, $k_N(2000, 1) \simeq 145$, $k_N(3000, 1) \simeq 225$), whereas for fixed N_{\max} change of s (for $s \neq 1$) enlarges the value of k_N [for example, $k_N(2000, 0.2) \simeq 1945$ and $k_N(2000, 5) \simeq 630$]. In our experiment, for each s , we usually prepared $n_T = 3 \times 10^6$ successful tours to simulate chains of the maximal length $N_{\max} = 2000$. The Monte Carlo experiments have been performed on the computer machine HP SL230s Gen8 consisting of cluster of Intel(R) Xeon(R) CPU E5-2670@2.60 GHz processing units. The program has been parallelised writing the code in OpenMP Fortran, and, for instance, 620 h of the CPU time have been used to simulate chains of the maximal length $N_{\max} = 2000$ with $s = 0.2$ in a run of $n_T = 3 \times 10^6$ successful tours.

For each specific s , from measured quantities $[W_N]_i$ and $[R_N^2]_i$, one can calculate their representative means obtaining Z_N and $\langle R_N^2 \rangle$. To evaluate these quantities and their standard errors, we applied the block analyses [34]. Within such an analysis the number of successful tours is divided into M blocks (indexed with $j = 1, 2, \dots, M$), each containing $s_N^{(j)} \simeq s_N/M$ samples of SAW, generated from $s_0^{(j)} \simeq s_0/M$ starting SAWs. For each block, one calculates the means $\langle W_N \rangle^{(j)}$ and $\langle R_N^2 \rangle^{(j)}$, ($j = 1, 2, \dots, M$), in accordance with Eqs. (8) and (9), respectively. The block means $\langle W_N \rangle^{(j)}$ (as well as $\langle R_N^2 \rangle^{(j)}$) are statistically independent, because different blocks contain SAW samples belonging to different simulation tours. The final estimates, obtained after averaging over the block number, are

$$Z_N = \langle W_N \rangle = \frac{1}{M} \sum_{j=1}^M \langle W_N \rangle^{(j)},$$

$$\langle R_N^2 \rangle = \frac{1}{M} \sum_{j=1}^M \langle R_N^2 \rangle^{(j)}, \quad (11)$$

while their standard errors should be calculated as $\sigma_{\langle X \rangle} = \sqrt{\frac{1}{M-1} (\langle X^2 \rangle - \langle X \rangle^2)}$, where X stands for both W_N and R_N^2 , since the block means are mutually independent [34]. In our implementation, the choice $M = 32$ for block numbers provides reliable results for calculated averages and related errors.

First we analyze the stiffness dependance of metric critical exponent ν , defined by Eq. (6), for $N \gg 1$. In a real Monte Carlo experiment, we simulate SAWs and calculate $\langle R_N^2 \rangle$ for finite values of chain length N . In that case it is appropriate to define a sequence of effective (N dependent) end-to-end distance critical exponents $\nu_N = \frac{1}{2} d \ln \langle R_N^2 \rangle / d \ln N$ [35], which can be viewed as a set of finite size estimators for the

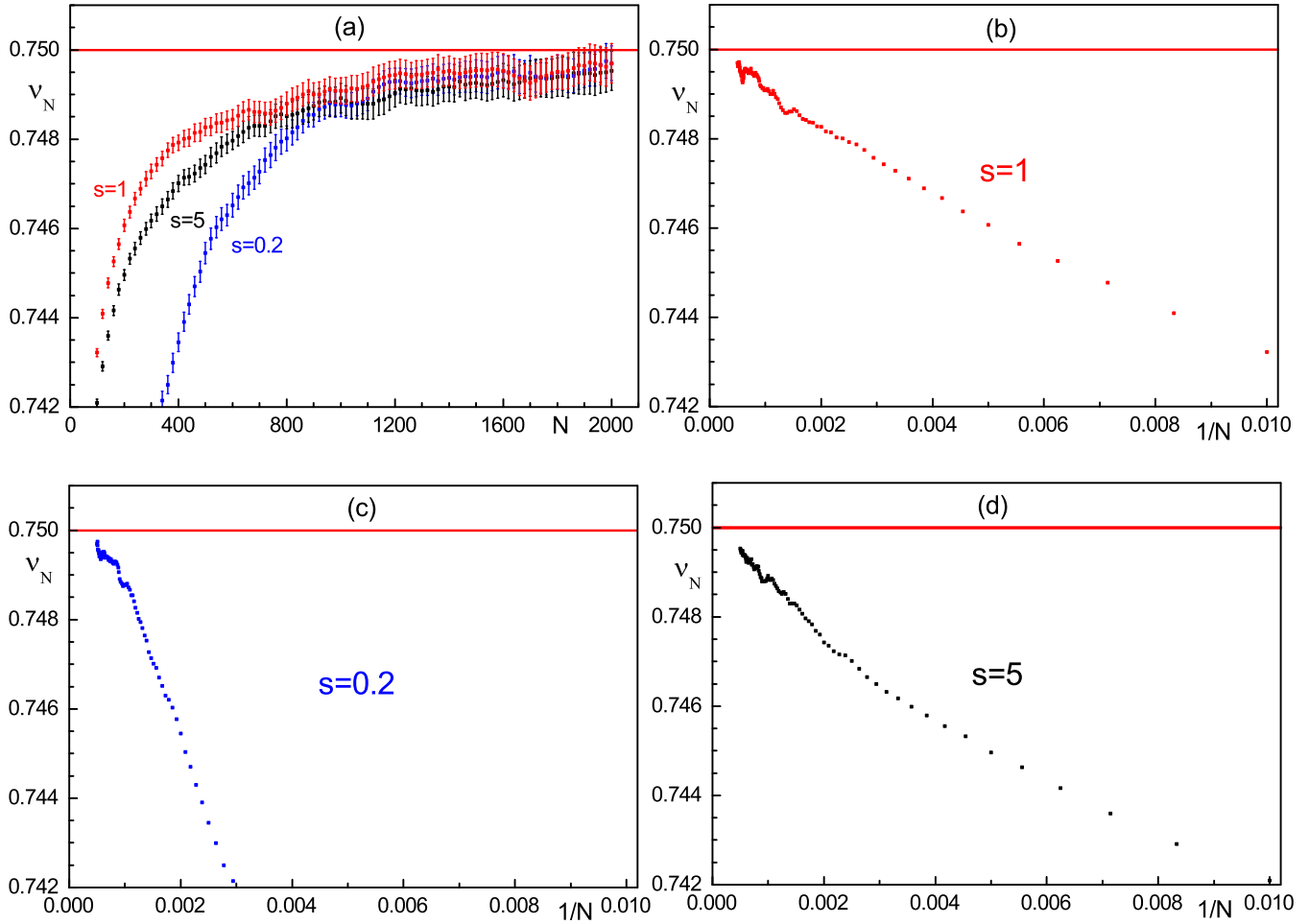


FIG. 2. (a) Results for the end-to-end distance critical exponent ν_N (together with associated standard errors) of semiflexible SAWs on the square lattice as a function of the polymer length N , for $s = 0.2, 1$, and 5 . Values of ν_N , given by Eq. (12), have been calculated with the step 2 for N , up to maximal length $N_{\max} = 2000$, and here we depicted only those with step 20 for N to distinguish the corresponding graph symbols. We note that graphs for the other studied values of s have similar shapes as graphs presented in this figure. Graphs for $s = 0.8, 0.6, 0.4, 0.3$, and $s = 1.5, 2, 3, 4$ lie gradually between corresponding graphs for $s = 1$ and 0.2 , and between $s = 1$ and 5 , respectively. Finally, in the cases (b)–(d) the values of ν_N are plotted as functions of $1/N$, for $s = 1, 0.2$, and 5 , when N runs from 100 to 2000. Red horizontal lines represent the value $3/4$.

end-to-end distance critical exponent ν . In practice, from quantities $\langle R_N^2 \rangle$ measured in the Monte Carlo simulations, the values of ν_N can be calculated [36–38] via the formula

$$\nu_N = \frac{1}{\ln 4} \ln \frac{\langle R_N^2 \rangle}{\langle R_{N/2}^2 \rangle}. \tag{12}$$

The obtained streams of ν_N estimators, for different values of s , are depicted in Fig. 2, as functions of N and $1/N$. We have shown only the results for fully flexible polymers $s = 1$, together with two opposite cases $s = 0.2$ and $s = 5$, since the graphs for the other studied values of s have similar shapes (see comment in caption of Fig. 2). In this figure one can see that, for each s , critical exponents ν_N , being always less than $3/4$, monotonically increase with the polymer length N . For shorter chains the polymer flexibility s affects the values of ν_N , while for larger N it seems that this dependence disappears. One also observes that the impact of s on ν_N is stronger for polymers with $s < 1$ than for ones with $s > 1$. To learn the precise limiting values of $\nu_N(s)$ (when $N \rightarrow \infty$), for

each specific s , we apply the following approach. Taking into account corrections to the scaling, the asymptotic form given by Eq. (6), for mean-squared end-to-end distance of SAW may be written as

$$\langle R_N^2 \rangle = AN^{2\nu} \left(1 + \frac{a_1}{N} + \frac{a_2}{N^2} + \dots + \frac{a'_0}{N^\Delta} + \frac{a'_1}{N^{\Delta+1}} + \dots \right). \tag{13}$$

The correction terms a_i/N^i are called analytical, whereas $a'_i/N^{\Delta+i}$ (with Δ not being an integer) are called nonanalytic (confluent) correction terms. For the square lattice the exponent Δ has the value $3/2$ [39–41], and the leading correction term is analytical. Combining Eqs. (12) and (13) we find that, in the region of large N , the set of effective critical exponents ν_N behaves as a linear function of $1/N$,

$$\nu_N = \nu - \frac{a_1}{\ln 4} \frac{1}{N}. \tag{14}$$

From data trends presented in Fig. 2, we perceive that for each s values of ν_N approach their limiting value ν from

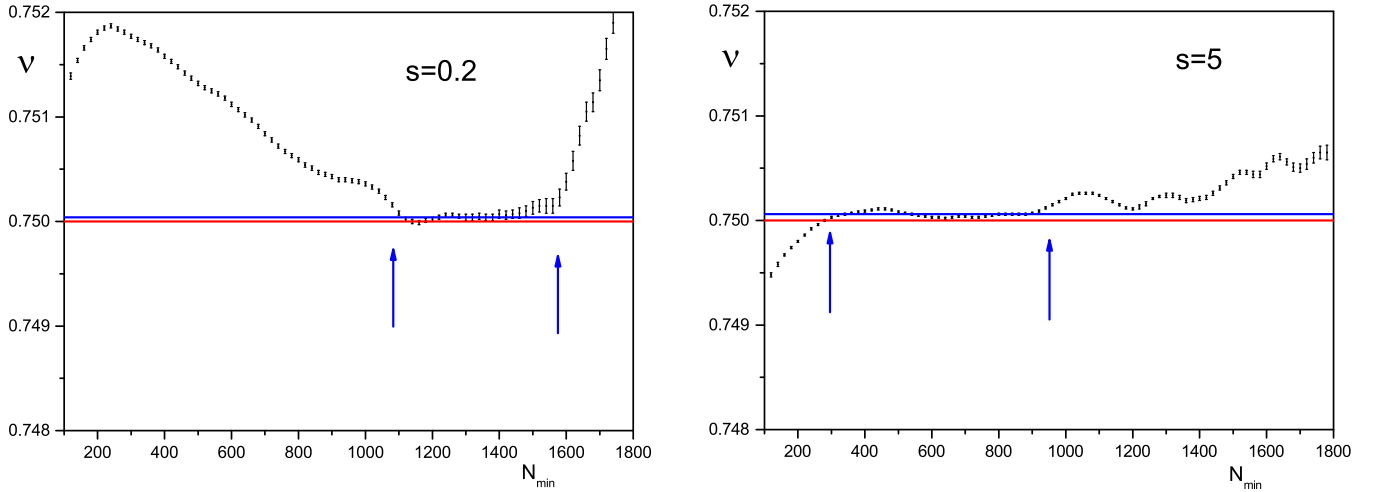


FIG. 3. Estimates of the critical exponent ν , as functions of N_{\min} (together with pertinent standard errors), obtained from weighted least squares linear fit of ν_N data (depicted in Fig. 2) for stiffness parameter values $s = 0.2$ and $s = 5$ of semiflexible SAWs. Blue arrows mark the sections for N_{\min} ([1100,1580] for $s = 0.2$, and [300,950] for $s = 5$) where values for ν look visually stable. Blue horizontal lines denote average values of data in marked sections, while red ones represent the value $3/4$.

below, when N increases. This implies a positive value for the coefficient a_1 . Also, we see that ν may be evaluated as the fitting line intersection of the vertical axis.

To get a sequence of estimates for ν , we form sets of data $\{1/N, \nu_N\}$, with N in the range $N \in [N_{\min}, N_{\max}]$. The windows $[N_{\min}, N_{\max}]$ are formed systematically [42–44], changing the lower bound N_{\min} from 20 to 1800, with step 2, and keeping the upper bound fixed $N_{\max} = 2000$. Next, we have prepared the weighted least squares linear fit of each set of data (labeled by N_{\min}), obtaining thereby series of estimates $\nu(N_{\min})$ for the critical exponent ν . Graphical presentations of the $\nu(N_{\min})$ data, for $s = 0.2$ and 5, are shown in Fig. 3. To get the final estimate we use the technique applied in Ref. [42]. We observe the section $[N_1, N_2]$ of N_{\min} where the $\nu(N_{\min})$ data visually appear stable, and in that range we average those data obtaining the first assessment $\nu^{(1)}(s)$ of metric critical

exponent. We repeat the whole procedure K times (for instance, $K = 17$ for $s = 0.2$ and $K = 11$ for $s = 5$) performing new series of n_T successful simulation tours. If in some series the function $\nu(N_{\min})$ is not stable (or the range of stability is too narrow) we do not include this simulation run into analysis. As result, we obtain K assessments $\nu^{(i)}(s)$, $i = 1, \dots, K$, of $\nu(s)$. Here we remark that choices of visually stable sections $[N_1, N_2]$ of data plots are subjective and lead to different values of confidence intervals for $\nu^{(i)}(s)$. Of course, estimates for $\nu^{(i)}(s)$ which are extracted from wider stable sections are more reliable, and this fact has been taken into account giving an additional weight (proportional to the size of $[N_1, N_2]$) to each $\nu^{(i)}(s)$, in corresponding data analysis. The final result

TABLE I. Numerical estimation of critical exponents ν , γ and the growth constant μ , for examined values of stiffness parameter s in case of the square lattice. The numbers in the brackets represent single standard errors concerning the last two digits. For instance, in the case of $s = 0.2$ the reading of ν should be: $\nu = 0.75010(16) \equiv 0.75010 \pm 0.00016$.

s	ν	γ	μ
0.2	0.75010(16)	1.3463(11)	1.3354846(09)
0.3	0.75014(12)	1.3450(11)	1.5009681(07)
0.4	0.75024(12)	1.3441(03)	1.6653779(29)
0.6	0.75016(09)	1.3430(02)	1.9917894(19)
0.8	0.75008(06)	1.3430(03)	2.3158270(08)
1	0.74999(02)	1.3430(04)	2.6381582(15)
1.5	0.74991(06)	1.3429(06)	3.4389711(16)
2	0.74985(11)	1.3439(06)	4.2351728(48)
3	0.74988(05)	1.3433(10)	5.8199005(78)
4	0.74985(08)	1.3417(06)	7.3988309(45)
5	0.75001(09)	1.3429(07)	8.9745048(82)

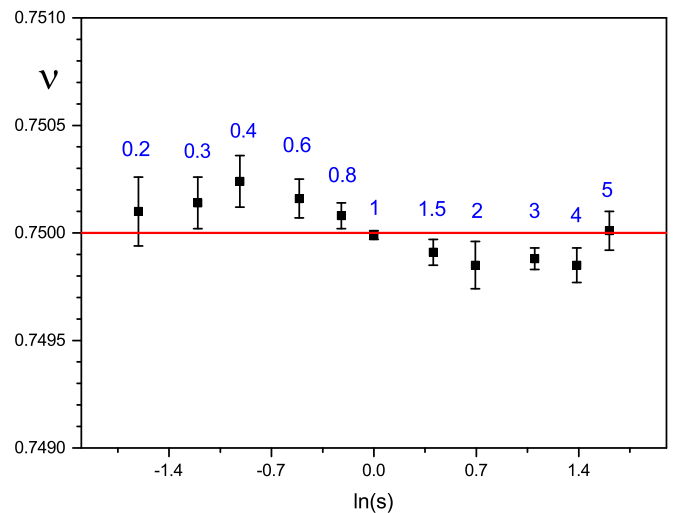


FIG. 4. Results for the end-to-end distance critical exponent ν of semiflexible SAW on the square lattice as a function of the logarithm of stiffness parameter s . Red horizontal line represents the value $3/4$, whereas the numbers above the data and their error bars correspond to the values of s .

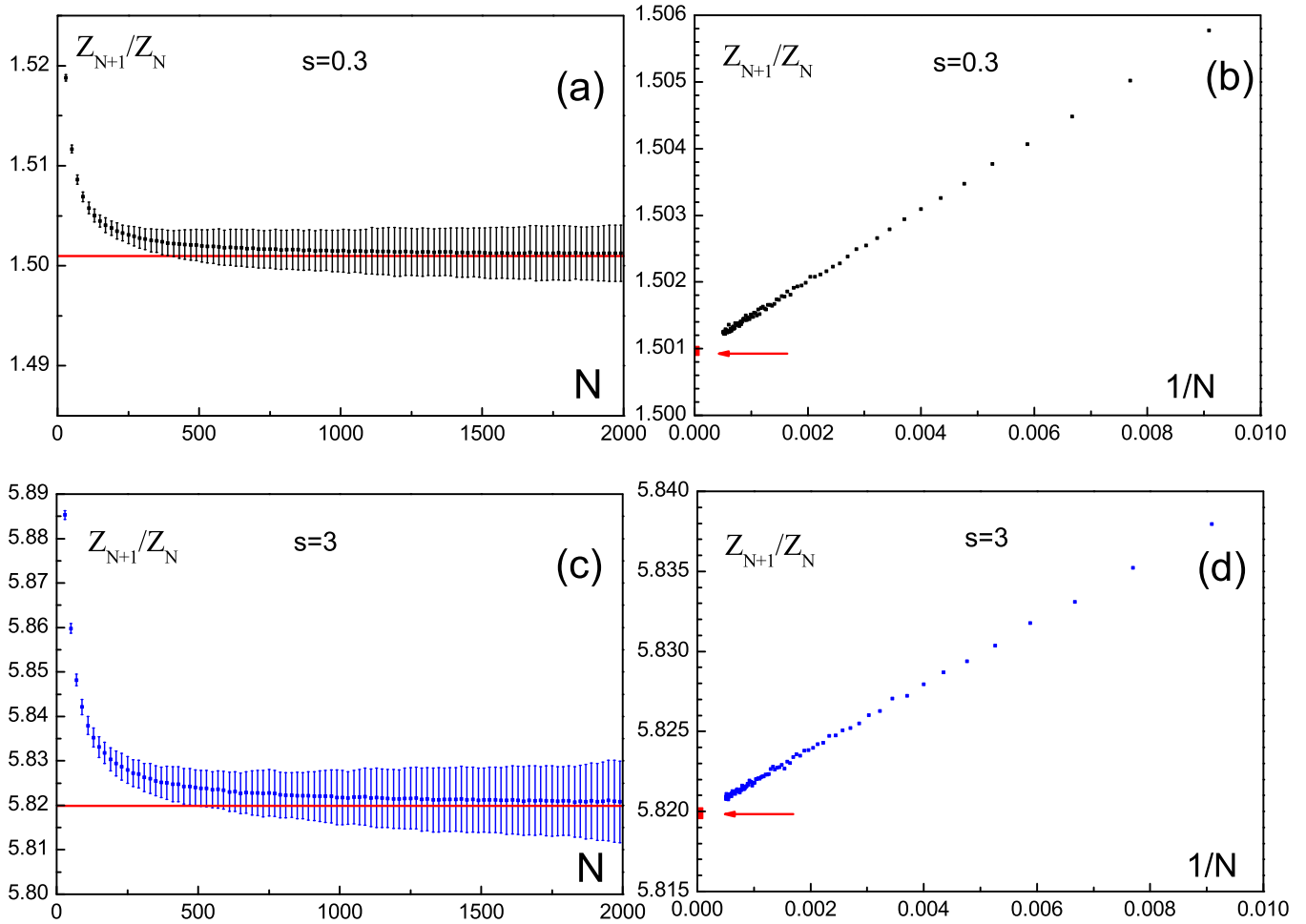


FIG. 5. Results for Z_{N+1}/Z_N (with their error bars) of semiflexible SAWs on the square lattice as a function of the SAW length N [parts (a) and (c) of the figure] and $1/N$ [parts (b) and (d)] for the stiffness parameters $s = 0.3$ and 3 . The ratio Z_{N+1}/Z_N , has been calculated with step 1 for N , up to maximal value 1999. To distinguish neighboring data on the graph, we plot them with step 20 for N . Red horizontal arrows (and lines) designate the corresponding linear extrapolations of data (quoted in Table I).

for $\nu(s)$, together with accompanied statistical errors, we find as a weighted mean of $\nu^{(i)}(s)$ ($i = 1, \dots, K$). Results for $\nu(s)$ are listed in Table I. Here we note that, besides the correction term $1/N$, we tried to include the next one [from Eq. (13)] in fitting model, but the range of stability for $\nu(N_{\min})$ was too narrow, so that we could not obtain any enhancement.

In a discussion of obtained values for ν (Table I), one can note that our Monte Carlo value of $\nu = 0.74999(2)$ for fully flexible polymers ($s = 1$) agrees very well with the exact result $3/4$, deviating 0.0013% from it. To examine the obtained results as a function of s , in Fig. 4 we have plotted ν against $\ln(s)$. One can see that for each s , exponent ν is very close to the value $3/4$, implying that polymer stiffness does not change the value of the metric critical exponent. Also, this graph suggests that estimates of ν for $s < 1$ are slightly increased in comparison with those for larger $s \geq 1$. This effect is a consequence of persistence length enlarging for polymers with $s < 1$ and will be elaborated with more details later (when we discuss the exponent γ).

Continuing our study of critical behavior of semiflexible SAWs on the square lattice we analyze the partition function Z_N , to extract information about μ and γ . Taking into account

correction to the scaling for large N , partition function can be written in the form

$$Z_N = B\mu^N N^{\gamma-1} \times \left(1 + \frac{b_1}{N} + \frac{b_2}{N^2} + \dots + \frac{b'_0}{N^\Delta} + \frac{b'_1}{N^{\Delta+1}} + \dots\right), \quad (15)$$

where the exponent Δ (a positive noninteger) governs nonanalytical correction terms [41]. To assess the studied quantities, we analyze the ratio [30,45]

$$\frac{Z_{N+1}}{Z_N} = \mu \left(1 + \frac{\gamma-1}{N} + \frac{q_1}{N^{\Delta+1}} + \frac{q_2}{N^2} + \dots\right), \quad (16)$$

whereupon it follows that on $1/N$ scale the leading correction is expressed by the linear term (since for the square lattice $\Delta = 3/2$). In our Monte Carlo experiment, for each specific s we have been able to estimate the value of Z_N [according to Eqs. (8) and (11)] and consequently to calculate the ratio given by Eq. (16). For instance, for $s = 0.3$ and 3 , the obtained data, in one experiment run (consisting of $n_T = 3 \times 10^6$ successful tours), are depicted in Fig. 5. As one can perceive from

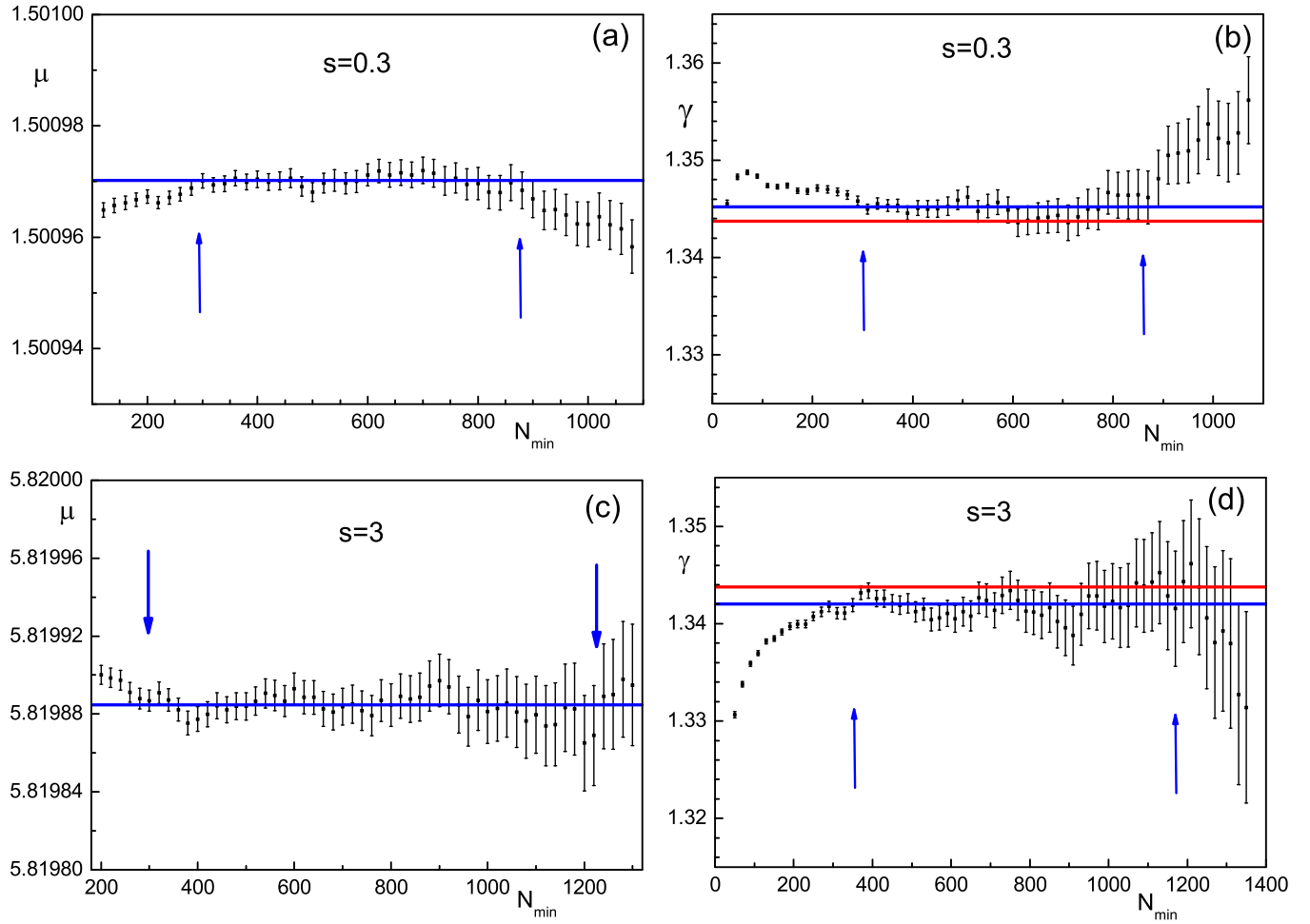


FIG. 6. Numerical assessment (for one simulation run) of the growth constant μ and critical exponent γ (with related error bars) as functions of N_{\min} , obtained from weighted least-squares linear fit of Z_{N+1}/Z_N against $1/N$, for $s = 0.3$ and 3. Blue arrows represent the interval for N_{\min} where data appear to be stable (blue horizontal lines represent average values of data embraced by corresponding intervals). The final estimates (given in Table I) for μ and γ are obtained as an average across K runs (we took $K = 23$ for $s = 0.3$, and $K = 7$ for $s = 3$), whose examples in these plots are presented, and for which one can notice very stable data behavior in a fairly wide region of N_{\min} . Red horizontal lines (on right panels) denote the value $43/32$.

Figs. 5(b) and 5(d), the function dependence $\frac{Z_{N+1}}{Z_N}(\frac{1}{N})$ is linear. Preparing the weighted linear fit of Z_{N+1}/Z_N against $1/N$, we can evaluate simultaneously both quantities of interest μ and γ . As in the case of critical exponent ν , we constituted the groups of data $\{1/N, Z_{N+1}/Z_N\}$ (with N in the range $N \in [N_{\min}, N_{\max}]$, where N_{\min} increases gradually and N_{\max} is fixed) to obtain the sequence of estimates for μ and γ via the corresponding fitting procedure for each set.

First, we present results obtained for the growth constant μ . For one simulation run, an example of set estimates $\mu(N_{\min})$ is plotted in Fig. 6(a), for polymers with $s = 0.3$, as well as in Fig. 6(c) for $s = 3$. Following procedure described in the case of ν evaluation, we have repeated simulations carrying out sufficient number of independent runs, and the final result we have calculated as an average over estimates obtained by all runs. Our definite Monte Carlo findings for $\mu(s)$ (together with accompanied statistical errors) are given in Table I. The growth constant μ governs the exponential increase of the partition function [see Eq. (3)], and consequently via the free energy per step $f = -k_B T \lim_{N \rightarrow \infty} \frac{\ln Z_N}{N} = \frac{\epsilon}{\ln s} \ln \mu$

determines thermodynamics of the system under study. From the last formula follows $\mu(s) = s^{f(s)/\epsilon}$, which means that in general μ is determined by the Boltzmann factor s , and may exceed the coordination number of the lattice, especially at low temperatures (for $s > 1$). The constant μ has explicit physical meaning only for $s = 1$ (i.e., in high temperature region). In this case $Z_N(s = 1)$ matches up with the total number C_N of distinct N -step SAWs: $Z_N(s = 1) = \sum_{N_b=0}^{N-1} C(N, N_b) = C_N$. Since for large N the ratio C_{N+1}/C_N approaches $\mu(s = 1)$, it follows that $\mu(s = 1)$ represents the average number of steps available to the walker having already completed a large number of steps (which cannot be larger than 3, for SAW on the square lattice). Our result 2.6381582(15), learned for flexible polymers ($s = 1$), is in a good agreement with the very precise numerical value $\mu = 2.63815853032790(3)$, calculated recently via the topological transfer-matrix method [46]. Also, it is more accurate than $\mu = 2.63818(3)$ [45] obtained using the similar method (flatPERM) simulating walks of the length up to 512. In Fig. 7(a) we plotted μ as a function of the stiffness parameter s , from

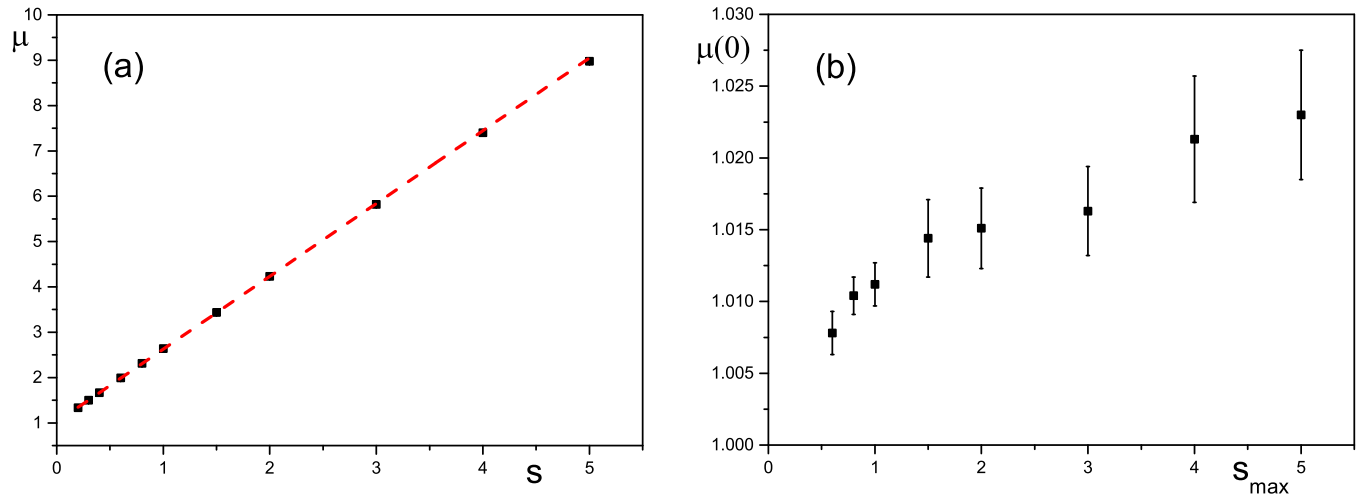


FIG. 7. (a) The growth constant μ (see Table I) of semiflexible SAWs on the square lattice, as a function of stiffness parameter s . Error bars are not depicted since they are smaller than the corresponding square symbols. Red dashed line is the weighted linear fit of the plotted data in the studied range of s . (b) Estimates (with the related error bars) of the growth constant $\mu(s = 0)$, as a function of s_{\max} , obtained from weighted linear fit of data (μ, s) , for s in the range $[0.2, s_{\max}]$.

where one may notice that, in the studied region of s , the growth constant μ is a monotonically increasing function of s . Furthermore, it seems that $\mu(s)$ is a linear function of stiffness parameter s for semiflexible SAWs on the square lattice. The same linear dependence of μ on the stiffness parameter s has been also observed in the fractal-to-Euclidean crossover region, for semiflexible polymers (with $0 < s \leq 1$) situated on the plane-filling fractal family [24], as well as for directed semiflexible SAWs on Euclidean lattices [18]. Finally, we discuss a possible behavior of $\mu(s)$, for very stiff chains $s \ll 1$. The weighted linear fit of data in Fig. 7(a) yields $\mu(s = 0) = 1.0230(45)$. To make a better assessment of $\mu(s = 0)$, we have performed a set of weighted linear fits of μ against s , for s in the range $[0.2, s_{\max}]$, lowering the upper bound s_{\max} from 5 to 0.6. The obtained results for $\mu(s = 0)$ as function of s_{\max} , are presented in Fig. 7(b), from where one can see that $\mu(s = 0)$ (being always larger than one) monotonically decreases, when s_{\max} decreases. Since this trend supports the expectation that μ should approach 1 when $s \rightarrow 0$ [as a first assessment, the simple linear extrapolation of data from Fig. 7(b), for $s_{\max} \leq 1$, gives $\mu(s = 0) = 1.0031(23)$], we infer that for very small s function $\mu(s)$ is not linear. Much the same behavior of μ , as a function of polymer flexibility, has been observed in the case of semiflexible compact polymer chains (modeled by Hamiltonian walks) on the four-simplex lattice [25], where the deviation from linearity has been observed only for very stiff chains ($s \ll 1$).

Eventually, to make our analysis of semiflexible SAWs on the square lattice complete, we discuss obtained values for γ (see Table I). First, we analyze the case of fully flexible polymers. The result for $\gamma(s = 1)$ has been evaluated from two-parameter linear fit (simultaneously estimating both μ and γ). The quoted value of $\gamma(s = 1)$ may be improved after fixing the growth constant at the most accurate value achieved so far $\mu = 2.63815853032790(3)$ [46], and then applying one-parameter fit. In this way we get more precise estimate $\gamma(s = 1) = 1.3433(02)$, which deviates 0.034% from the exact value

$43/32 = 1.34375$. Next, to assess the influence of parameter s on γ behavior, in Fig. 8 we have shown the values of γ , as a function of $\ln(s)$. From this plot it is quite clear that for $s \geq 1$ exponent γ does not depend on s , but for $s < 1$ one cannot immediately conclude the same. In the latter region it is visible that values of γ are slightly increased in comparison with the values for larger s , and therefore an additional analysis is necessary to draw a definite conclusion about its dependence on s . We believe that increase of γ values for smaller s (in our plot it is visible for $s \leq 0.4$) comes from the fact that in this region the systematic error in γ estimation (produced by neglecting higher order terms in the fitting model) is larger

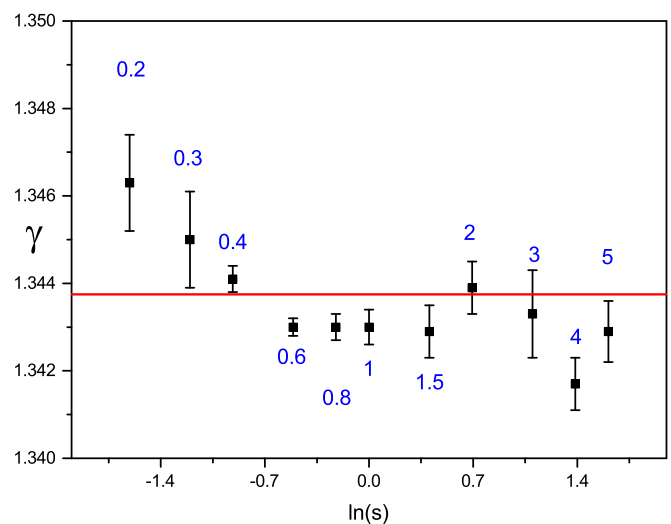


FIG. 8. Results for the critical exponent γ of semiflexible SAWs on the square lattice as a function of the logarithm of stiffness parameter s . Red horizontal line represents the value $43/32$, whereas the numbers above or below the data and their error bars correspond to the specific values of s .

comparing with one produced for larger s . This assumption may be supported by the following arguments. Since the persistence length for $s = 0.2$ is 5 times larger than for $s \geq 1$, it follows that effective number of steps $N_{\text{eff}} = Ns$ (this is the number of steps measured in the persistence length units), for $N = 2000$ and $s = 0.2$, is $N_{\text{eff}} = 400$. This implies that systematic error in γ evaluation, for $s = 0.2$ and $N = 2000$, could be compared with one obtained for $s \geq 1$ and $N = 400$. To check that, for $s = 1$, we recalculated γ , fitting only data up to $N_{\text{max}} = 400$, and obtained the value 0.14% larger than one obtained for $N_{\text{max}} = 2000$ (given in Table I). The obtained increase of γ for $s = 1$, caused by reduction in N_{eff} , is comparable with 0.19% for which is $\gamma(s = 0.2) = 1.3463$ larger than $43/32$. We expect the same outcome in calculation of γ for smaller values of s , where diminished N_{eff} produces a systematic increase in γ estimates. For this reason, to obtain more accurate estimates for smaller values of s one should simulate polymers with larger number of steps (for $s = 0.2$ the maximal length of polymer should be $N_{\text{max}} = 10\,000$), and also large enough number of samples have to be created. We have tried to increase the maximal number of steps up to $N_{\text{max}} = 3\,000$, but created graphs, similar to those in Fig. 6, have not been stable, so that obtained data have not been useful for further examination.

On the whole, regarding both critical exponents ν and γ , we may say that obtained numerical results are consistent with the universality arguments based prediction that the SAW bending energy ϵ is irrelevant for the SAW critical exponents on Euclidean lattices, and its only effect is in changing the persistence length. Our investigation is the first numerical study of semiflexible polymers on Euclidean lattices which confirms numerically the universality arguments assumption about critical exponents behavior of semiflexible SAWs. So far, this behavior of semiflexible SAWs on homogeneous lattices was demonstrated explicitly only for directed semiflexible SAWs [18], using the scaling method. However, in contrast to the case of homogeneous lattices, disorder in nonhomogeneous lattices combined with the stiffness, in some cases can constrain the persistence length, and consequently induces

dependence of critical exponents on s [19]. This behavior has been observed in a study of semiflexible polymers on the plane-filling fractal family, where we have also found that in fractal-to-Euclidean crossover region critical exponents do not depend on s , but their values are different from the Euclidean ones [24].

IV. SUMMARY AND CONCLUSION

We have studied the semiflexible linear polymer chains modeled by self-avoiding random walk (SAW) on the square lattice by applying the PERM Monte Carlo simulation method. Varying the stiffness parameter s of the chain we have calculated numerically the critical exponents ν (associated with the mean squared end-to-end distances of polymer chain) and γ (associated with partition function of polymer chain system), as well as the growth constant μ . Our results show that for finite polymer chain length effective values of critical exponent ν are stiffness dependent functions, while for very long chains we find a clear numerical evidence that both critical exponents (ν and γ) do not depend on the polymer flexibility. Furthermore, we have found that the growth constant μ displays a linear dependence of s , in the studied region.

The performed research has been made for a limited set of polymer flexibility parameter values, and it would be worth to expand it. To this end it is desirable to initiate additional investigations using, for instance, some temperature-independent Monte Carlo methods, like flatPERM [32] or multi-canonical chain-growth algorithm [47], which could be more efficient for studying the statistics of stiffer chains. Also, it would be interesting to extend this study to the case of polymers situated on three-dimensional Euclidean lattices.

ACKNOWLEDGMENT

This research has been performed as a part of the work within Project No. 171015 funded by the Ministry of Education, Science, and Technological Development of the Republic of Serbia.

-
- [1] N. Madras and G. Slade, *The Self-Avoiding Walk* (Birkhäuser, Boston, 1993).
 - [2] C. Vanderzande, *Lattice Models of Polymers* (Cambridge University Press, Cambridge, 1988).
 - [3] C. Bustamante, J. F. Marko, E. D. Siggia, and S. Smith, *Science* **265**, 1599 (1994).
 - [4] C. K. Ober, *Science* **288**, 448 (2000).
 - [5] K. Binder, H.-P. Hsu, and W. Paul, *Eur. Phys. J. Special Topics* **225**, 1663 (2016).
 - [6] J. P. Berezney, A. B. Marciel, C. M. Schroeder, and O. A. Saleh, *Phys. Rev. Lett.* **119**, 127801 (2017).
 - [7] I. M. Storm, M. A. Cohen Stuart, R. de Vries, and F. A. M. Leermakers, *Phys. Rev. E* **97**, 032501 (2018).
 - [8] M. Zhang and A. H. E. Müller, *J. Polym. Sci., Part A: Polym. Chem.* **43**, 3461 (2005).
 - [9] S. S. Sheiko, B. S. Sumerlin, and K. Matyjaszewski, *Prog. Polym. Sci.* **33**, 759 (2008).
 - [10] P. J. Flory, *Proc. R. Soc. London A* **234**, 60 (1956).
 - [11] P. J. Flory, *Statistical Mechanics of Chain Molecules* (Interscience, New York, 1969).
 - [12] J. W. Halley, H. Nakanishi, and R. Sundararajan, *Phys. Rev. B* **31**, 293 (1985).
 - [13] S. B. Lee and H. Nakanishi, *Phys. Rev. B* **33**, 1953 (1986).
 - [14] V. Privman and S. Redner, *Z. Phys. B* **67**, 129 (1987).
 - [15] J. Moon and H. Nakanishi, *Phys. Rev. A* **44**, 6427 (1991).
 - [16] V. Privman and H. L. Frisch, *J. Chem. Phys.* **88**, 469 (1988).
 - [17] V. Privman and N. M. Švrakić, *J. Stat. Phys.* **50**, 81 (1988).
 - [18] V. Privman and N. M. Švrakić, *Directed Models of Polymers, Interfaces, and Clusters: Scaling and Finite-Size Properties*, Lecture Notes in Physics 338 (Springer-Verlag, Berlin, Heidelberg, 1989).
 - [19] A. Giacometti and A. Maritan, *J. Phys. A* **25**, 2753 (1992).
 - [20] H.-P. Hsu, W. Paul, and K. Binder, *Europhys. Lett.* **92**, 28003 (2010).

- [21] V. Blavatska, K. Haydukivska, and Yu. Holovatch, *Ukr. J. Phys.* **57**, 41 (2012).
- [22] H.-P. Hsu, W. Paul, and K. Binder, *Europhys. Lett.* **95**, 68004 (2011).
- [23] G. F. Tuthill and W. A. Schwalm, *Phys. Rev. B* **46**, 13722 (1992).
- [24] I. Živić, S. Elezović–Hadžić, and S. Milošević, *Phys. Rev. E* **80**, 061131 (2009).
- [25] D. Lekić and S. Elezović–Hadžić, *Physica A* **390**, 1941 (2001).
- [26] B. Nienhuis, *Phys. Rev. Lett.* **49**, 1062 (1982).
- [27] B. Duplantier, *Phys. Rev. Lett.* **57**, 941 (1986).
- [28] P. Grassberger, *Phys. Rev. E* **56**, 3682 (1997).
- [29] M. N. Rosenbluth and A. W. Rosenbluth, *J. Chem. Phys.* **23**, 356 (1955).
- [30] A. Rechnitzer and E. J. Janse van Rensburg, *J. Phys. A* **35**, L605 (2002).
- [31] J. Batoulis and K. Kremer, *J. Phys. A* **21**, 127 (1988).
- [32] T. Prellberg and J. Krawczyk, *Phys. Rev. Lett.* **92**, 120602 (2004).
- [33] H.-P. Hsu, V. Mehra, W. Nadler, and P. Grassberger, *J. Chem. Phys.* **118**, 444 (2003).
- [34] E. J. Janse van Rensburg, *The Statistical Mechanics of Interacting Walks, Polygons, Animals and Vesicles*, 2nd ed. (Oxford University Press, Oxford, 2015).
- [35] B. Li, N. Madras, and A. D. Sokal, *J. Stat. Phys.* **80**, 661 (1995).
- [36] T. Prellberg, *J. Phys. A* **34**, L599 (2001).
- [37] A. Bedini, A. L. Owczarek, and T. Prellberg, *J. Phys. A* **46**, 085001 (2013).
- [38] E. J. Janse van Rensburg, *J. Stat. Mech.* (2016) 033202.
- [39] A. R. Conway and A. J. Guttmann, *Phys. Rev. Lett.* **77**, 5284 (1996).
- [40] I. Jensen, *J. Phys. A* **37**, 5503 (2004).
- [41] S. Caracciolo, A. J. Guttmann, I. Jensen, A. Pelissetto, A. N. Rogers, and A. D. Sokal, *J. Stat. Phys.* **120**, 1037 (2005).
- [42] Y. Chan and A. Rechnitzer, *J. Phys. A* **45**, 405004 (2012).
- [43] N. Clisby and B. Dünweg, *Phys. Rev. E* **94**, 052102 (2016).
- [44] N. Clisby, *J. Phys. A* **50**, 264003 (2017).
- [45] A. L. Owczarek and T. Prellberg, *J. Phys. A* **41**, 375004 (2008).
- [46] J. L. Jacobsen, C. R. Scullard, and A. J. Guttmann, *J. Phys. A* **49**, 494004 (2016).
- [47] M. Bachmann and W. Janke, *Phys. Rev. Lett.* **91**, 208105 (2003).